FABRICATION AND STUDY OF OPTICAL PROPERTIES OF TERNARY ZnTeS SEMICONDUCTOR QUANTUM DOTS

Thi Minh Thuy Nguyen[1,*]

[1]*Faculty of Physics, Thai Nguyen University of Education*

Abstract

Ternary $ZnTe_{1-x}S_x$ ($0 \leq x \leq 1$) semiconductor quantum dots (QDs) with varying x composition were successfully fabricated by a wet chemical method in ODE solvent. Their crystal structure, oscillation characteristics, and optical properties were studied through X-ray diffraction patterns (XRD), Raman (RS), absorption spectra (Abs), and photoluminescence (PL). The results showed that ternary $ZnTe_{1-x}S_x$ QDs have the zinc-blende (ZB) structure when x changes. When changing x composition, the emission wavelength of ternary $ZnTe_{1-x}S_x$ QDs can change from 408 nm to 526 nm. Evidence of ternary $ZnTe_{1-x}S_x$ QDs with uniform Se and S compositions was studied and proven through XRD patterns and RS scattering spectra.

Keywords: *Ternary; semiconductor; quantum dots; optical properties;* $ZnTe_{1-x}S_x$.

1. Introduction

Quantum dots (QDs) are nanoscale semiconductor particles that exhibit unique optical and electronic properties due to quantum confinement effects [1]-[3]. These properties include size-dependent photoluminescence, high quantum yield, and tunable bandgap energies [2], [4]. As a result, QDs have been widely explored for applications in optoelectronics, photovoltaics, bio-imaging, and sensing. Traditional binary QDs such as CdS, CdSe, CdTe, ZnS, ZnSe,… have been extensively studied [5]-[8]. However, ternary QDs have emerged as an attractive alternative due to their enhanced flexibility in tailoring electronic and optical properties [3], [5], [6]. Ternary semiconductor QDs, including CdTeSe, CdTeS, CdSSe, ZnCdS, and ZnCdSe consist of three different atomic elements, enabling more precise control over bandgap engineering [9]-[12]. The incorporation of a third component allows for fine-tuning of emission wavelengths, increased stability, and improved quantum efficiency compared to binary counterparts [9], [11]. Ternary QDs exhibit unique structural and optical properties due to the interplay between different constituent elements. The introduction of an additional component enables bandgap engineering, allowing for continuous tuning of emission wavelengths across the visible and near-infrared spectrum [10]. These QDs offer intermediate bandgaps and enhanced carrier mobility, making them ideal candidates for various applications [10]-[12].

* Corresponding author, email: thuyntm@tnue.edu.vn
DOI: 10.56651/lqdtu.jst.v3.n01.951.pce

Despite the many advantages, the fabrication of ternary QDs still faces some difficulties and challenges such as: (i) photo-oxidation and thermal degradation affect the long-term performance of QDs, (ii) the presence of cadmium raises environmental and biological concerns, requiring the study of environmentally friendly alternatives, and (iii) large-scale synthesis with uniform quality remains a challenge for commercial applications. Therefore, this study focuses on the development of cadmium-free materials and enhancement of the quantum yield of ternary QDs. In this study, the author fabricated ternary $ZnTe_{1-x}S_x$ ($0 \leq x \leq 1$) QDs by wet chemical method in non-bonding solvent ODE. The size and crystal structure of the QDs were investigated by an UV-Vis and XRD. The results showed that the ternary $ZnTe_{1-x}S_x$ ($0 \leq x \leq 1$) QDs have size of about 3 nm and ZB structure when x changes. By fixing the size and only changing the x ratio, the PL spectral peak of the ternary $ZnTe_{1-x}S_x$ ($0 \leq x \leq 1$) QDs changes in a wide range from 408 nm to 526 nm. The formation of ternary QDs with uniform composition distribution is demonstrated by Raman scattering spectrum and linear change of crystal lattice constant with x ratio.

2. Experiment

2.1. Chemical

Aldrich chemicals for the preparation of ternary $ZnTe_{1-x}S_x$ QDs include: ZnO powder (99.99%), Te powder (99.99%), S powder (99.98%), 1-octadecene (ODE, 90%), oleic acid (OA, 90%). Chemicals used for centrifugation to clean and disperse the QDs is ethanol, isopropanol and toluene purchased from Chinese companies.

2.2. Fabrication of $ZnTe_{1-x}S_x$ quantum dots

The mixture of ZnO, ODE, and OA was stirred at 400 rpm at 210°C for 1 hour. Once the solution turned lemon yellow, indicating Zn^{2+} ion formation, it was kept as solution 1. In parallel, Te and S powders were dissolved in ODE at 200°C for 3 hours with continuous stirring at 400 rpm, yielding solution 2. The injection of solution 2 into solution 1 was performed rapidly (within ~5 seconds) at 280°C under a nitrogen atmosphere to induce instantaneous nucleation. The reaction was maintained for 90 minutes at this temperature. Afterward, the system was allowed cool to room temperature. Rapid injection helps control nucleation and size uniformity, while the controlled cooling process reduces thermal strain on the QDs. The $ZnTe_{1-x}S_x$ QDs are centrifuged to remove ligands and unreacted Zn^{2+}, Te^{2-} and S^{2-} precursors for subsequent characterization measurements.

2.3. Characterization

The crystal structure of the QDs was investigated by X-ray diffractometer

(Siemens D-5005). Fluorescence and Raman scattering spectra were measured by LabRam HR800 (Horriba, Jobin Yvon) with 325 nm excitation wavelength of He-Cd laser. Optical absorption spectra were measured by Jasco 770 (Varian). Photoluminescence was measured using an FLS1000 spectrophotometric system equipped with a 450 W Xe lamp.

3. Results and discussion

The EDX spectrum was used to analyze the elemental composition of the ternary $ZnTe_{1-x}S_x$ ($0 \leq x \leq 1$) QDs (x = 0.3, 0.5, and 0.7) and is presented in Fig. 1.

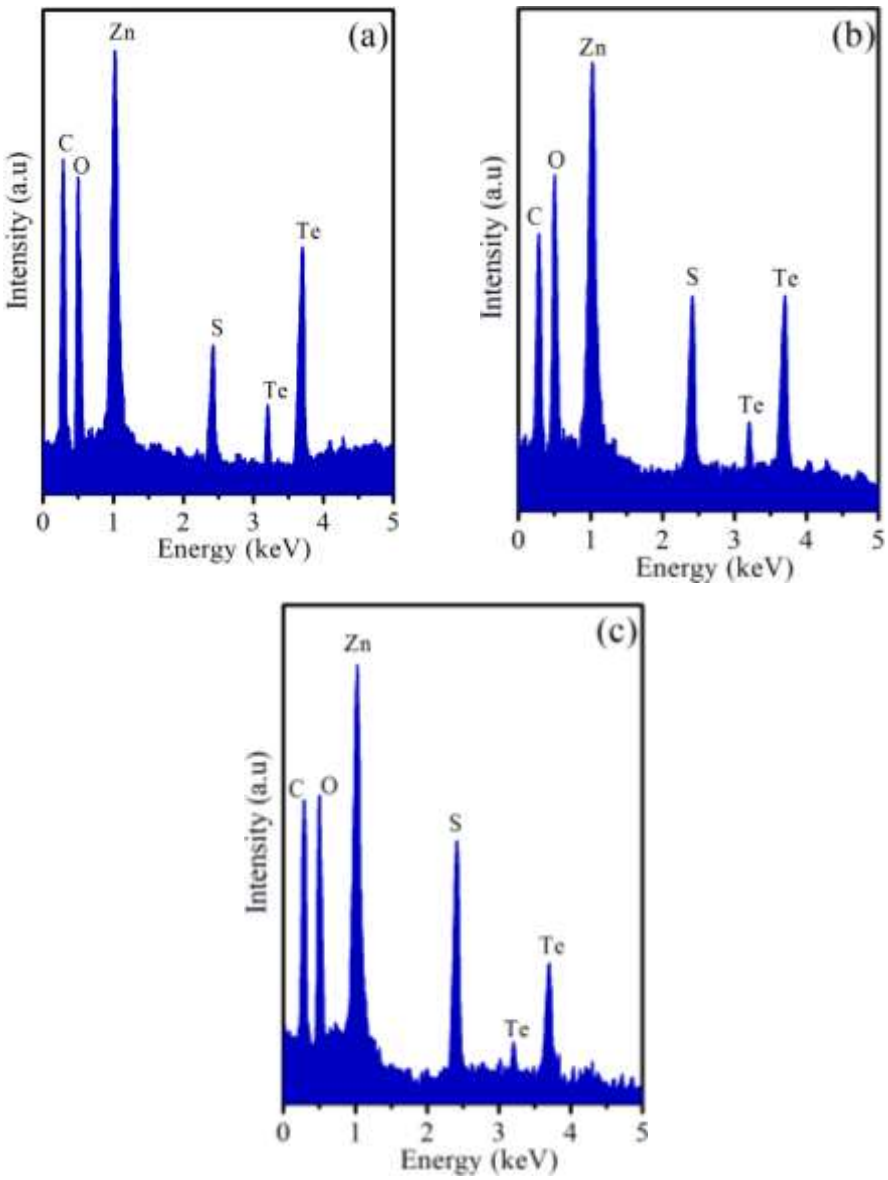

Fig. 1. The EDX spectra of nanocrystals: (a) $ZnTe_{0.7}S_{0.3}$, (b) $ZnTe_{0.5}S_{0.5}$, and (c) $ZnTe_{0.3}S_{0.7}$.

The elemental composition was determined in terms of atomic and weight percentages. Distinct characteristic peaks corresponding to the elements C, O, Zn, Te, and S were observed in the EDX spectrum. The results in Tab. 1 indicate that the actual Te/S ratio involved in the reaction is higher than the theoretically calculated ratio, demonstrating that Te exhibits higher chemical reactivity than S. This property is crucial for the synthesis of ternary QDs containing both S and Te. The elemental composition of all samples, as obtained from the EDX spectra, is summarized in Tab. 1.

Tab. 1. The composition of the atomic (%) of ternary $ZnTe_{1-x}S_x$ (x = 0.3, 0.5, 0.7) QDs

Sample	**Atomic (%)**		
	Zn	**Te**	**S**
$ZnTe_{0.7}S_{0.3}$	48.12	38.69	13.19
$ZnTe_{0.5}S_{0.5}$	46.54	29.96	23.5
$ZnTe_{0.3}S_{0.7}$	45.09	19.77	35.14

To demonstrate the formation of ternary $ZnTe_{1-x}S_x$ QDs, the author measured their Raman (RS) scattering spectra, the results are observed in Fig. 2. The RS spectra of ZnTe and ZnS QDs clearly observed the 1LO peaks at wavenumbers 208 and 347 cm^{-1}. The 1LO peaks of these QDs were shifted to lower wavenumbers compared to the 1LO peaks of bulk semiconductors ZnTe and ZnS [13], [14]. The observed shift of the 1LO peaks to lower wavenumbers in ZnTe and ZnS QDs compared to their bulk counterparts (210 cm^{-1} for ZnTe and 350 cm^{-1} for ZnS) is primarily due to quantum confinement, phonon confinement, strain, and surface effects [15]. These factors collectively modify the phonon dispersion and lead to the redshift observed in Raman spectroscopy [13], [15]. The well-defined 2LO vibrational peaks of ZnTe and ZnS QDs observed at wavenumbers 414 cm^{-1} and 690 cm^{-1}, respectively, indicate the high crystalline quality of these QDs. For ternary $ZnTe_{1-x}S_x$ QDs, the 1LO Raman peaks appeared at 324, 279, and 248 cm^{-1}, corresponding to compositions of x = 0.7, 0.5, and 0.3, respectively. These Raman peaks are located between those of ZnS QDs (347 cm^{-1}) and ZnTe QDs (208 cm^{-1}), consistent with the bandgap of ternary $ZnTe_{1-x}S_x$ QDs lying between the bandgaps of ZnTe and ZnS QDs. Furthermore, no 1LO peaks corresponding to pure ZnTe or ZnS were detected in the Raman spectrum of ternary $ZnTe_{1-x}S_x$ QDs, suggesting the absence of phase-separated ZnTe or ZnS QDs and ruling out the formation of ZnTe/ZnS or ZnS/ZnTe core/shell structures in solution.

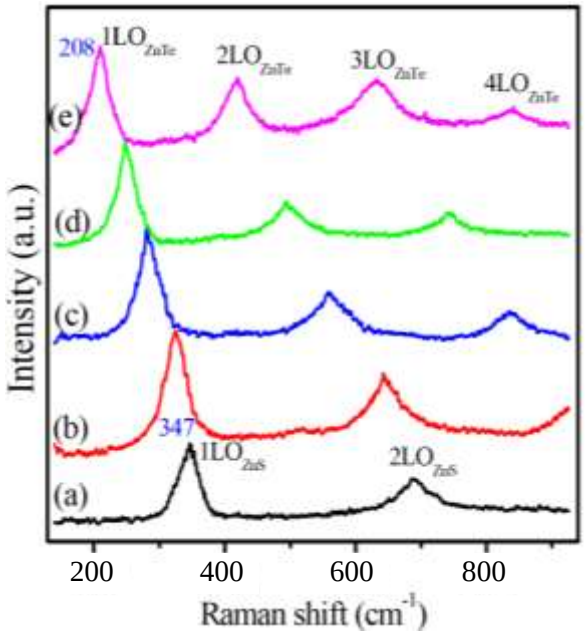

Fig. 2. RS spectra of ternary $ZnTe_{1-x}S_x$ ($0 \leq x \leq 1$) QDs.

As x varies, the crystal structure of ternary $ZnTe_{1-x}S_x$ ($0 \leq x \leq 1$) QDs was investigated using XRD, as observed in Fig. 3. The broad diffraction peaks in the samples are attributed to the nanoscale size of the $ZnTe_{1-x}S_x$ QDs and the strain induced within the QDs. All samples exhibit a zinc blende (ZB) structure, confirmed by the presence of three diffraction peaks corresponding to the (111), (220), and (311) lattice planes [16]. For x = 0, the observed diffraction peaks for the NC $ZnTe_{1-x}S_x$ match the peak positions of ZnTe (JCPDS#01-0582), and for x = 1 they align with the peak positions of ZnS (JCPDS#80-0020) [17], [18]. The crystallite size *D* of the QDs was calculated using the Debye-Scherrer formula [16], [17]:

$$D = \frac{k\lambda}{\beta\cos\theta} \tag{1}$$

where λ = 0.154 nm is the X-ray wavelength, k = 0.9 is the Scherrer constant, β is the full width at half maximum (FWHM) of the diffraction peak, and θ is the diffraction angle. The lattice constant *a* of the QDs was determined from XRD data using the following equation [16], [17]:

$$\frac{1}{d_{hkl}^2} = \frac{h^2 + k^2 + l^2}{a^2} \tag{2}$$

where *d* is the interplanar spacing corresponding to the Miller indices (*h*, *k*, *l*), and is calculated using Bragg's equation [16], [17]:

$$n\lambda = 2d_{hkl}\sin\theta \quad (3)$$

The diffraction peak positions gradually shift toward larger θ values as x increases. This shift is due to the greater substitution of S ions (small radius) for Te ions (larger radius). The observed shift in the diffraction peaks of ternary $ZnTe_{1-x}S_x$ ($0 \le x \le 1$) QDs suggests the formation of a homogeneous alloy structure rather than a mere physical mixture of NC ZnTe and ZnS. Lattice parameters and crystallite size of ternary $ZnTe_{1-x}S_x$ QDs are observed in Tab. 2. In this study, the author use the parameters of the diffraction peak (111), which is the peak with the largest intensity.

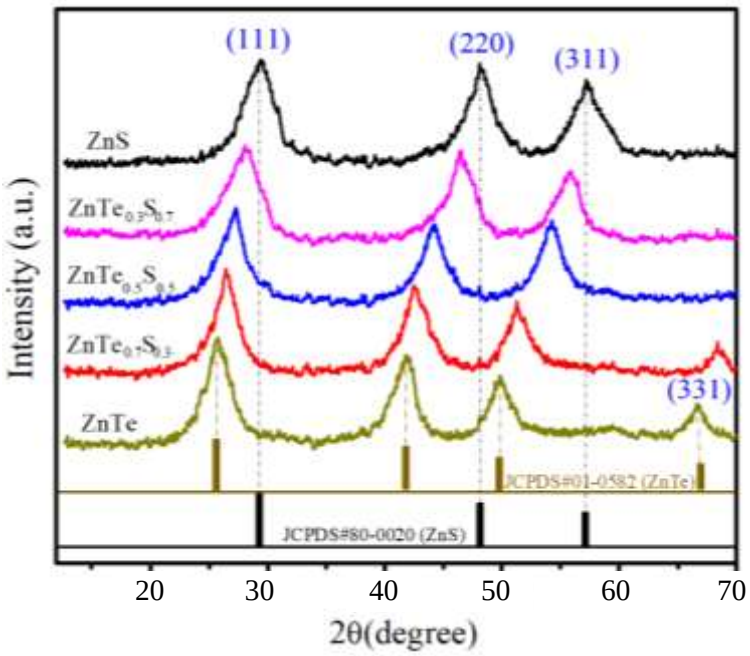

Fig. 3. XRD patterns of ternary $ZnTe_{1-x}S_x$ ($0 \le x \le 1$) QDs.

Tab. 2. Lattice parameters and crystallite size of ternary $ZnTe_{1-x}S_x$ ($0 \le x \le 1$) QDs

Sample	**2θ (°)**	**d_{hkl} (nm)**	**a (nm)**	**β (°)**	**D (nm)**
ZnTe	25.76	0.352	0.610	3.02	2.69
$ZnTe_{0.7}S_{0.3}$	26.51	0.345	0.597	2.98	2.73
$ZnTe_{0.5}S_{0.5}$	27.34	0.330	0.571	3.05	2.68
$ZnTe_{0.3}S_{0.7}$	28.23	0.326	0.564	3.53	2.32
ZnS	29.43	0.315	0.545	3.21	2.56

The optical absorption spectra of ZnTe, ZnS, and ZnTeS QDs were recorded (Fig. 4) to investigate their electronic transitions and bandgap properties. The absorption spectra of these QDs exhibit distinct features corresponding to their quantum confinement effects and compositional variations. The absorption peak of pure ZnTe QDs is observed at 481 nm, corresponding to a bandgap of approximately 2.57 eV. This is blue-shifted compared to the bulk ZnTe bandgap (~2.26 eV) due to the quantum confinement effect [9], [16]. The absorption peak of pure ZnS QDs is observed at 334 nm, corresponding to a bandgap of approximately 3.71 eV. For QDs, when the particle size decreases below this exciton radius, the bandgap increases due to electron-hole confinement. Using the Brus equation, the bandgap energy for a QDs can be estimated as [16], [19]:

$$E_{QD} = E_{bulk} + \frac{\hbar^2 \pi^2}{2R^2}\left(\frac{1}{m_e^*} + \frac{1}{m_h^*}\right) - \frac{1.8e^2}{4\pi\varepsilon_0\varepsilon_r R} \quad (4)$$

where E_{QD} is the band gap of the QD with radius R. E_{bulk} is the bulk band gap energy (2.26 eV for ZnTe, 3.6 eV for ZnS). $\hbar$ is the reduced Planck's constant. m_e^* is the effective mass of the electron in ZnTe, ZnS ($m_e^* \approx 0.12\ m_0$ for ZnTe, $m_e^* \approx 0.24\ m_0$ for ZnS where m_0 is the free electron mass). m_h^* is the effective mass of the hole in ZnTe, ZnS ($m_h^* \approx 0.6\ m_0$ for ZnTe, $m_h^* \approx 0.86\ m_0$ for ZnS). ε_0 is the permittivity of free space. ε_r is the relative permittivity of ZnTe, ZnS ($\varepsilon_r \approx 10.2$ for ZnTe, $\varepsilon_r \approx 8.3$ for ZnS), e is the elementary charge [16], [17]. The estimated sizes of ZnTe, ZnS QDs corresponding to a bandgap energy of 2.57 eV and 3.71 are approximately 3.1 nm and 3.08 nm, respectively.

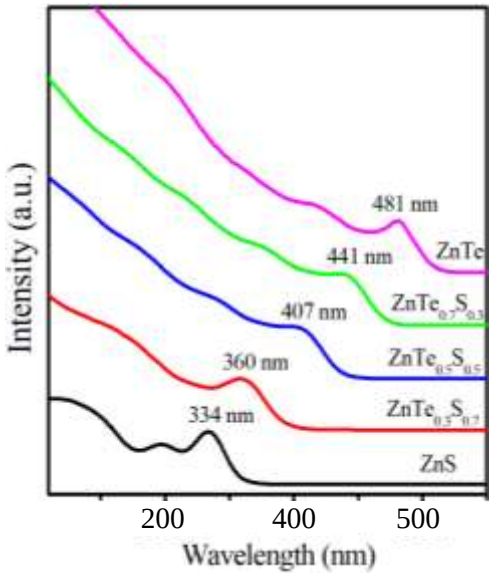

Fig. 4. UV-vis absorption (Abs) of ternary $ZnTe_{1-x}S_x$ ($0 \leq x \leq 1$) QDs.

The Te/S ratio significantly influences the emission wavelength of the QDs. Fig. 5 presents the photoluminescence (PL) spectra of ternary $ZnTe_{1-x}S_x$ ($0 \le x \le 1$) QDs. The PL spectrum of ZnS QDs exhibits an excitonic emission peak at 408 nm, which originates from the recombination of conduction band electrons with valence band holes [16], [19]. In addition to the excitonic emission peak, ZnS QDs also display another emission peak around 556 nm. This secondary peak is attributed to impurity states, lattice defects, and/or surface states [9], [19]. As the Te/S ratio increases from 0 to 1, the emission peaks shift toward the red region (from 408 nm to 526 nm), similar to the absorption spectra. The Te/S ratio not only affects the emission wavelength of the QDs but also influences their quantum yield (QY).

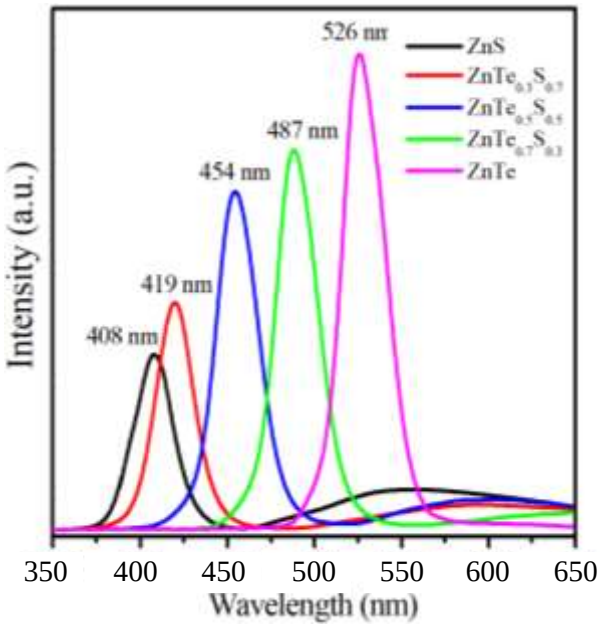

Fig. 5. PL spectra of ternary $ZnTe_{1-x}S_x$ ($0 \le x \le 1$) QDs.

QY is a crucial parameter for evaluating the luminescence efficiency of a material. The PL QY of a sample is determined by comparison with an organic dye with a known QY, and the calculation is performed using the following equation [19], [20]:

$$QY_{NC} = QY_{dye} \frac{I_{NC}}{I_{dye}} \left(\frac{n_{NC}}{n_{dye}} \right)^2 \frac{1-10^{-OD_{dye}}}{1-10^{-OD_{NC}}} \quad (5)$$

where I represents the integrated emission intensity of the PL spectrum, obtained by fitting the PL spectrum using a combination of Gaussian and Lorentzian functions. The parameter n denotes the refractive index, while OD represents the optical density of the QDs or the dye sample. It is important to note that the organic dye used in this study is

Rhodamine 6G, which has a QY of 95% when dissolved in ethanol [20]. The calculated results indicate that as *x* increases from 0 to 1, the PLQY decreases from 34.65% to 19.43%. This result is also consistent with the PLQY of some other ternary semiconductor compounds such as CdTeSe, CdZnSe [9], [12], [20]. The observed decrease in PLQY from 34.65% for ZnTe to 19.43% for ZnS as x increases can be attributed to several physical and chemical factors. First, the higher ionic character of ZnS compared to ZnTe leads to more surface defects and trap states, which act as non-radiative recombination centers. Second, lattice mismatch between $Te^{2-}$and S^{2-}ions introduces strain and alloy disorder, creating localized states within the bandgap. Third, stronger quantum confinement in S-rich QDs reduces electron-hole overlap, thus lowering radiative recombination probability. Moreover, differences in surface passivation efficiency between Te-rich and S-rich QDs may also contribute to the reduced QY. These combined effects result in a decrease in QY of the $ZnTe_{1-x}S_x$ QDs. The optical parameters of the samples are observed in Tab. 3. The tunable fluorescence emission confirms the alloying effect between ZnS and ZnTe. This characteristic makes these materials suitable for optoelectronic applications such as LEDs, lasers, and bio-imaging.

Tab. 3. Optical parameters of ternary $ZnTe_{1-x}S_x$ ($0 \le x \le 1$) QDs

Sample	Abs peak (nm)	PL peak (nm)	E_g (eV)	QY (%)
ZnTe	481	526	2.57	34.65
$ZnTe_{0.7}S_{0.3}$	441	487	2.81	28.12
$ZnTe_{0.5}S_{0.5}$	407	454	3.04	26.09
$ZnTe_{0.3}S_{0.7}$	360	419	3.44	22.49
ZnS	334	408	3.71	19.43

4. Conclusion

The ternary $ZnTe_{1-x}S_x$ QDs with varying x ratios were successfully synthesized via a wet-chemical method using a non-coordinating ODE solvent. The formation of a homogeneous alloy structure with uniform composition distribution was confirmed through RS spectroscopy and XRD analysis. The RS spectra revealed the presence of the 1LO Raman peak of $ZnTe_{1-x}S_x$ QDs in the wavenumber range of 208-347 cm^{-1}. The results showed that the ternary $ZnTe_{1-x}S_x$ QDs had zinc-blende (ZB) structure and

particle size of about 3 nm as x varied. The PL emission peak of ternary $ZnTe_{1-x}S_x$ QDs was tuned over a broad range from 408 nm to 526 nm. With the capability of tuning emission wavelengths over such a wide range, ternary $ZnTe_{1-x}S_x$ QDs hold significant potential for applications in optoelectronic devices and bioimaging. These applications benefit from stable emission in the visible range and compatibility with water-soluble surface modifications.

Acknowledgement

This research was funded by the Ministry of Education and Training under the project number B2025-TNA-02.

References

[1] V. Biju *et al.*, "Semiconductor quantum dots and metal nanoparticles: Syntheses, optical properties, and biological applications", *Analytical and Bioanalytical Chemistry*, Vol. 391, pp. 2469-2495, 2008. DOI: 10.1007/s00216-008-2185-7

[2] H. S. Mansur, "Quantum dots and nanocomposites", *Wiley Interdisciplinary Reviews: Nanomedicine and Nanobiotechnology*, Vol. 2, Iss. 2, pp. 113-129, 2010. DOI: 10.1002/ wnan.78

[3] B. Bajorowicz *et al.*, "Quantum dot-decorated semiconductor micro- and nanoparticles: A review of their synthesis, characterization, and application in photocatalysis", *Advances in Colloid and Interface Science*, Vol. 256, pp. 352-372, 2018. DOI: 10.1016/j.cis.2018.02.003

[4] K. He *et al.*, "CdS QDs: Facile synthesis, design and application as an "on-off" sensor for sensitive and selective monitoring Cu^{2+}, Hg^{2+} and Mg^{2+} in foods", *Food Chemistry*, Vol. 390, 2022. DOI: 10.1016/j.foodchem.2022.133116

[5] J. Zhang *et al.*, "Identification of facet-dependent coordination structures of carboxylate ligands on CdSe nanocrystals", *Journal of the American Chemical Society*, Vol. 141, pp. 15675-15683, 2019. DOI: 10.1021/jacs.9b07836

[6] H. Wu *et al.*, "Optical properties of CdTe quantum dots in silicate glasses containing CaO", *Optical Materials*, Vol. 148, 2024. DOI: 10.1016/j.optmat.2024.114897

[7] S. G. B. Passos *et al.*, "Paired electrosynthesis of ZnSe/ZnS quantum dots and Cu^{2+} detection by fluorescence quenching", *Journal of Luminescence*, Vol. 228, 2020. DOI: 10.1016/j.jlumin.2020.117611

[8] S. Sudheer Khan *et al.*, "Construction of ZnS QDs decorated gC_3N_4 nanosheets for enhanced catalytic degradation of Rhodamine B", *Ceramics International*, Vol. 50, No. 19, pp. 36479-36486, 2024. DOI: 10.1016/j.ceramint.2024.07.033

[9] H. T. Van *et al.*, "Synthesis and optical properties of tunable dual emission copper doped $CdTe_{1-x}Se_x$ alloy nanocrystals", *Optical Materials*, Vol. 97, 2019. DOI: 10.1016/j.optmat.2019.109392

[10] H. T. Van *et al.*, "Effects of ligand and chemical affinity of S and Se precursors on the shape, structure and optical properties of ternary $CdS_{1-x}Se_x$ alloy nanocrystals", *Materials Letters*, Vol. 264, 2020. DOI: 10.1016/j.matlet.2020.127387

[11] W. Fan *et al*., "Facile synthesis of ZnCdS quantum dots via a novel photoetching MOF strategy for boosting photocatalytic hydrogen evolution", *Separation and Purification Technology*, Vol. 330, Part A, 2024. DOI: 10.1016/j.seppur.2023.125258

[12] X. Jin *et al*., "Thick-shell CdZnSe/ZnSe/ZnS quantum dots for bright white light-emitting diodes", *Journal of Luminescence*, Vol. 229, 2021. DOI: 10.1016/j.jlumin.2020.117670

[13] J. Trajić *et al*., "Raman spectroscopy of ZnS quantum dots", *Journal of Alloys and Compounds*, Vol. 637, pp. 401-406, 2015. DOI: 10.1016/j.jallcom.2015.03.027

[14] B. B. Wang *et al.*, "Raman scattering and photoluminescence of zinc telluride nanopowders at room temperature", *Journal of Luminescence*, Vol. 131, Iss. 12, pp. 2550-2554, 2011. DOI: 10.1016/j.jlumin.2011.06.028

[15] S. Kumar *et al.*, "Origin of the high-frequency shoulder in the Raman spectra of CdSe quantum dots", *The Journal of Physical Chemistry Letters*, Vol. 15, Iss. 41, pp. 10392-10398, 2024. DOI: 10.1021/acs.jpclett.4c02335

[16] N. T. M. Thuy *et al.*, "Er^{3+} and Sm^{3+} co-doped ZnS quantum dots: Judd-Ofelt, luminescent properties and energy transfer", *Journal of Luminescence*, Vol. 255, 2023. DOI: 10.1016/j.jlumin.2022.119538

[17] E. R. Shaaban *et al.*, "Microstructural parameters and optical constants of ZnTe thin films with various thicknesses", *Physica B: Condensed Matter*, Vol. 404, Iss. 20, pp. 3571-3576, 2009. DOI: 10.1016/j.physb.2009.06.002

[18] L. Kashinath *et al.*, "Sol-gel assisted hydrothermal synthesis and characterization of hybrid ZnS-RGO nanocomposite for efficient photodegradation of dyes", *Journal of Alloys and Compounds*, Vol. 695, No. 25, pp. 799-809, 2017. DOI: 10.1016/j.jallcom.2016.10.063

[19] T. T. T. Huong *et al.*, "Eu^{3+}-doped ZnO quantum dots: Structure, vibration characteristics, optical properties, and energy transfer process", *Nanoscale Advances*, Vol. 7, pp. 909-921, 2025. DOI: 10.1039/D4NA00858H

[20] N. X. Ca *et al.*, "Controlling the optical and magnetic properties of CdTeSe and Gd-doped CdTeSe alloy semiconductor nanocrystals", *RSC Advances*, Vol. 13, pp. 36455-36466, 2023. DOI: 10.1039/D3RA06332A

CHẾ TẠO VÀ NGHIÊN CỨU TÍNH CHẤT QUANG CỦA CHẤM LƯỢNG TỬ BÁN DẪN BA THÀNH PHẦN ZnTes

Nguyễn Thị Minh Thủy[1]

[1]*Khoa Vật lý, Trường Đại học Sư phạm, Đại học Thái Nguyên*

Tóm tắt: Các chấm lượng tử bán dẫn (QD) ba thành phần $ZnTe_{1-x}S_x$ ($0 \le x \le 1$) có thành phần x thay đổi đã được chế tạo thành công bằng phương pháp hóa ướt trong dung môi ODE. Cấu trúc tinh thể, đặc trưng dao động và tính chất quang học của chúng đã được nghiên cứu thông qua các phép đo: Nhiễu xạ tia X (XRD), Raman (RS), phổ hấp thụ (Abs) và phát quang (PL). Kết quả nghiên cứu cho thấy các QD ba thành phần $ZnTe_{1-x}S_x$ đều có cấu trúc lập phương (ZB). Khi thành phần x thay đổi, bước sóng phát xạ của các QD ba thành phần $ZnTe_{1-x}S_x$ có thể thay đổi từ 408 nm đến 526 nm. Bằng chứng về các QD ba thành phần $ZnTe_{1-x}S_x$ có thành phần Te và S đồng nhất đã được nghiên cứu và chứng minh thông qua các giản đồ nhiễu xạ tia X và phổ tán xạ RS.

Từ khoá*: Ba thành phần; bán dẫn; chấm lượng tử; tính chất quang;* $ZnTe_{1-x}S_x$.

Received: 04/11/2024; Revised: 04/03/2025; Accepted for publication: 28/04/2025

❑